VERSITA

Growth of large SbSI crystals[*]

PIOTR SZPERLICH[1][†], BARTŁOMIEJ TOROŃ[1], MARIAN NOWAK[1], MARCIN JESIONEK[1],
MIROSŁAWA KĘPIŃSKA[1], WŁODZIMIERZ BOGDANOWICZ[2]

[1]Solid State Physics Section, Institute of Physics, Silesian University of Technology,
Krasińskiego 8, 40-019 Katowice, Poland

[2]Institute of Material Science, University of Silesia, 75 Pułku Piechoty 1A, 41-500 Chorzów, Poland

In this paper a novel method of SbSI single crystals fabrication is presented. In this method a sonochemically prepared SbSI gel is used as an intermediate product in a vapour growth process. The main advantages of the presented technique are as follows. First, the SbSI gel source material has lower temperature of sublimation and allows to avoid explosions during SbSI synthesis (the sonochemical synthesis is free of any explosion hazard). Second, but not least, the grown SbSI single crystals have smaller ratio of longitudinal and lateral dimensions. The cross sections of the presented crystals are relatively large (they are up to 9 mm^2). The crystals have been characterized by X-ray diffraction, angle-resolved optical spectroscopy, and diffusive reflectivity.

Keywords: *antimony sulfoiodide; crystal growth; vapour growth process; nanomaterials*

1. Introduction

The study of the class of ferroelectric-semiconductors of A^{V}B^{VI}C^{VII} type, wherein antimony sulfoiodide (SbSI) is the most outstanding representative, is of principal interest. SbSI has an unusually large number of interesting properties. Among them there are pyroelectric, pyrooptic, piezoelectric, electrooptic, and nonlinear optical effects. The main properties of SbSI were reviewed in a few monographs [1–6]. However, the properties of this material have been still investigated [7–13]. Due to these properties, SbSI is an attractive and suitable material for thermal imaging [3, 4, 14–17], light modulators [3, 4, 18], ferroelectric field effect transistors (FeFET) [19, 20], gas sensors [21], piezoelectric elements used in certain types of electromechanical transducers [4, 22–24], temperature autostabilized nonlinear dielectric elements (TANDEL) [25, 26], time-controlling devices [3, 4, 27] and other applications. Recently,

heterostructures fabricated by CO$_2$ laser treatment of SbSI single crystals have been produced [13, 28].

SbSI single crystals can be obtained by several different methods [29], for example using the melt or flux growth (slowly cooling and unidirectional solidification), vapour growth (sublimation-condensation and chemical transport reactions) and hydro-thermal method. Polycrystalline samples obtained from the melt consist of many needles. Monocrystalline samples having mirror-like surfaces were obtained from the vapour phase in a closed tube. Unfortunately, due to the anisotropy of the SbSI crystal structure the usually grown single crystals are remarkably needle-like along c-axis and with relatively small cross-sections. It limits the potential applications of SbSI. Bigger samples of hot-pressed SbSI bulk ceramics were prepared but their physical properties were not satisfying [30]. Recently, a laser-write method to form SbSI single crystal features on chalcogenide glasses for integration into infrared devices has been published [31]. SbSI can also be obtained in the form of nanocrystals. The ultrasound irradiation has been applied to induce the 1D growth
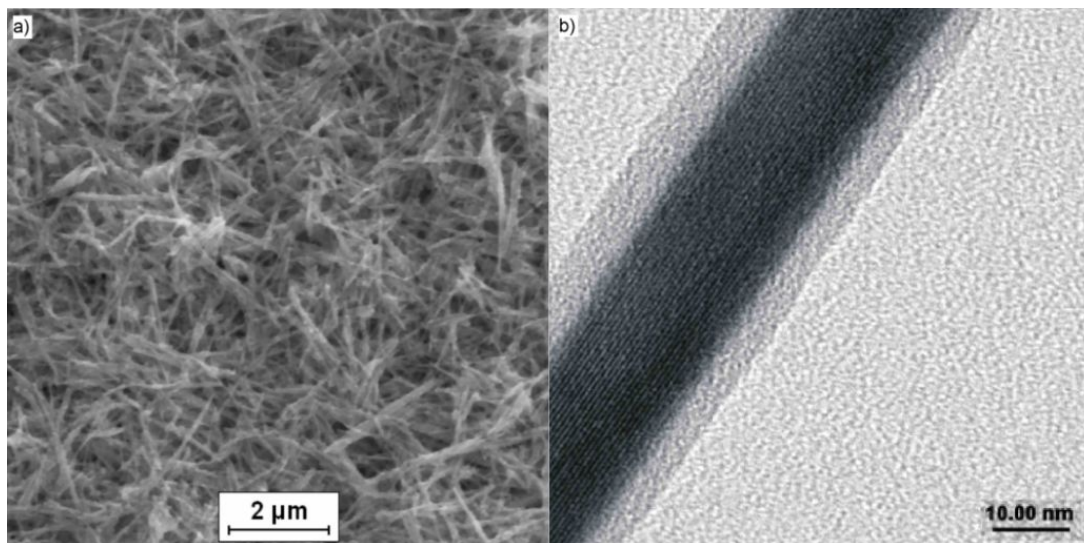

Fig. 1. SEM image of sonochemically prepared SbSI gel (a), and HRTEM image of single SbSI nanocrystal (b) [13].

of nanowires of ternary and quaternary chalco-halides formed from the group 15-16-17 elements (see [13, 32] and Refs. in [33]).

2. Growth and characterization of SbSI crystals

SbSI gel synthetized sonochemically was used as the input material to growth SbSI single crystals. SbSI gel was prepared from the constituents (the elements: antimony, sulphur and iodine) weighed in the stoichiometric ratio for SbSI. Ethanol was used as a solvent in the reaction. All reagents used in the experiment were analytically pure and were purchased from Sigma-Aldrich (antimony, 99.95 %) and from POCH S.A., Gliwice, Poland, (subli-mated sulfur (pure p.a.), iodine (pure p.a.), and ab-solute ethanol (pure p.a.)). In a typical procedure, antimony, sulfur and iodine with stoichiometric ra-tio were immersed at room temperature and am-bient pressure in absolute ethanol, which was con-tained in a Pyrex glass cylinder of 20 mm inside di-ameter. The closed cylinder was partly submerged in water in an ultrasonic reactor (InterSonic IS-UZP-2, frequency 35 kHz, with 80 W peak elec-trical power and 2 W/cm^2 power density guar-anteed by the manufacturer). The sonochemical

fabrication was carried out at 323 K. Obtained gel was ten times centrifuged to extract SbSI gel. Af-ter each rinsing the ethanol above, the sediment was substituted by the new, pure ethanol. At the end, SbSI gel was dried at room temperature and reduced pressure (100 Pa). As-prepared samples were made up of large quantity of single-crystalline nanowires with diameters of about 10 to 50 nm and lengths reaching up to several micrometres. SEM and HRTEM images of SbSI gel have been pre-sented in Fig. 1. Accurate information about the sonochemical synthesis process of SbSI gel and its characterization one can find in [13].

The growth process of SbSI single crystals from vapor phase was performed in closed termisil am-poules that were placed in a two-zone furnace. Temperature of every zone was controlled inde-pendently. Dried SbSI gel (80 g) was put into an ampoule of 150 mm length and 35 mm diameter and the ampoule was evacuated to the pressure of 10^{-2} Pa, and then it was sealed. The bottom and top of the ampoule were wrapped with aluminum foil in order to obtain uniform temperature at the source and crystallization zones. The suitable gra-dient of temperatures (between the source and crys-tallization zones) and the aluminum foil allowed the growth of large crystals only in the upper part

of ampoule. So prepared ampule was put in the furnace. The process was carried out in a horizontal position of the furnace. However, due to large amount of material inside the ampule, the furnace was tilted at a small angle (∼5 degrees) to avoid spontaneous material transport from the source to crystallization zone. Crystal growth was performed in variable temperature gradient. Temperature profile in the furnace has been shown in Fig. 2.
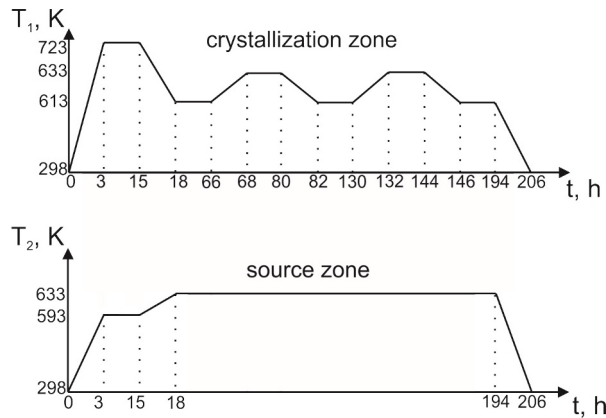

Fig. 2. Temperature profile in the furnace (description in the text).

At the beginning of the process the source zone was heated to 633 K, whereas the crystallization zone was heated to 723 K to evaporate the possible centers of nucleation in this part of ampule. Then, the cycles with changing temperature were applied in the crystallization zone (Fig. 2). As the temperature in crystallization zone was lower than the temperature in the source zone, the crystals growth was continued. After that, for a short time, the temperature in the crystallization zone was raised to induce evaporation of small, weak crystals. So called pendulum heating method has been reported in [34]. The cycle was repeated three times. The SbSI crystal growth was carried out for 206 hours. The maximal value of cross-section for obtained SbSI single crystals was about 9 mm^2 (Fig. 3).

Laue back reflection measurements were carried out to determine a crystalline structure of the grown SbSI single crystal. The measurements were performed at temperature of 295 K using Mo Kα radiation ($\lambda = 0.70926$ Å). The area of X-ray irradiation was 0.8 mm in diameter. The incidence

angle of X-rays upon (001) front plane was set to 6.5°. The crystal has been irradiated for 52.5 hours. So long exposure time is typical for semiconducting materials. Fig. 4 presents Laue back reflection photography registered from the (001) crystal plane (visible in Fig. 3). Crystal plane strips from orthogonal crystal planes have been indicated by straight lines. The obtained Laue back scattering photography shows that the examined sample is a single crystal. Reflexes from several crystal planes have also been identified (Fig. 4). The calculated lattice constants, a = 0.858 nm, b = 1.017 nm, c = 0.414 nm, are typical for Pnam crystal symmetry of paraelectric SbSI.
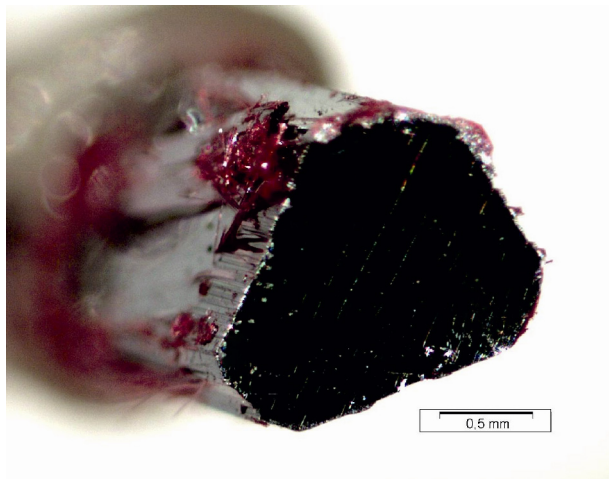

Fig. 3. Large SbSI single crystal grown in the experiment.

Fig. 5 shows typical hysteresis loops of polarization for SbSI crystal that were registered in a Sawyer-Tower circuit [35]. Measurements were performed for two orientations of electric field (E) relative to c-axis of SbSI single crystal (E∥c and E⊥c) and for temperature range of 283 K to 333 K. In the case of E⊥c no hysteresis loop has been observed even for high electric field (E$_{MAX}$ = 7.7 kV/cm). For E∥c one can see that the hysteresis loop evaluated for 283 K is well saturated, whereas for 333 K it almost declines (Fig. 5). Fast decrease of hysteresis loop area starts at a temperature of 292 K, which corresponds to Curie temperature (T$_C$) in SbSI [36]. The values of spontaneous polarization P$_s$ = 11.5 μC/cm^2, rema-
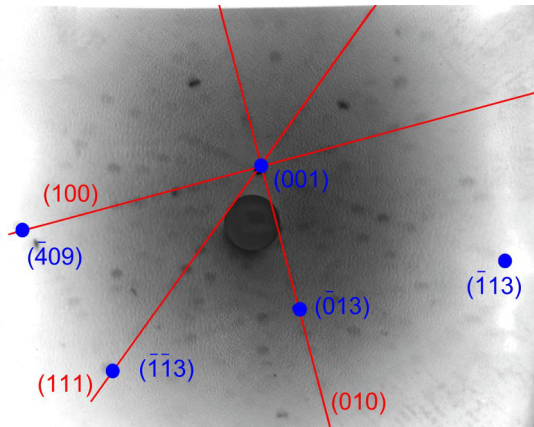
Fig. 4. Laue back scattering reflection photography from the grown SbSI single crystal with indicated orthogonal crystal planes strips and reflexes form crystal planes.

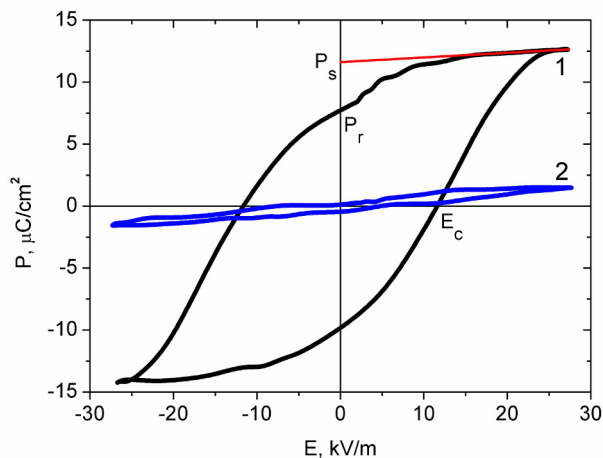
Fig. 5. Hysteresis loops of SbSI single crystal at temperatures 283 K (1) and 333 K (2) with indicated spontaneous polarization P_s, remanent polarization P_r, and the value of coercive field E_c (sample was biased parallel to the c axis of the crystal).

nent polarization $P_r = 7.7$ µC/cm², coercive field $E_c = 116$ V/cm, and energy required for sample repolarization $W = 5.19$ kJ/m³ at temperature 283 K (Fig. 5) have been determined.

Current-voltage characteristics were measured using Keithley 2410 C in temperature range of 283 K to 333 K for different orientations of electric field vector towards c-axis of SbSI single crystals (Fig. 6). One can see that the current density is significantly higher for E‖c than for E⊥c at every temperature. Furthermore, for E‖c and temperature lower than T_C, the current-voltage characteristics are typical of common ferroelectric crystals [37]. Arrows in Fig. 6a. represent the direction of current density changes. One can see that the singularity occurs in J(E) characteristics but only after repolarization. It is caused by charge release during domain reorientation. For the E⊥c singularities of J(E) characteristics are not visible even at high electric field (E = 7.7 kV/cm). This leads to a conclusion that polarization vector is parallel to c-axis of SbSI crystal.

Electrical conductivity (Fig. 7) of SbSI single crystals for E‖c and E⊥c has been determined from current-voltage characteristics measured in temperature range of 283 K to 333 K. The electrical conductivity is much higher for E‖c than for E⊥c. Arrhenius dependence has been fitted to the data presented in Fig. 7 to determine the activation energy (E_a) of electrical conductivity. The values of $E_a = 0.341(55)$ eV and $E_a = 0.236(22)$ eV have been determined for E⊥c in cases of ferroelectric and paraelectric phases of SbSI, respectively. The $E_a = 0.441(12)$ eV and $E_a = 0.339(22)$ eV have been established for E‖c in the same cases.

To determine the optical energy gap (E_g) of SbSI crystals the diffuse reflectance spectroscopy (DRS) has been applied [38]. Measurements were carried out using spectrophotometer SP-2000 equipped with an integrating sphere ISP-REF Ocean Optics Inc. The standard WS-1 Ocean Optics Inc. was used as a reference. Spectra were recorded for the planes perpendicular and parallel to c-axis of SbSI crystal at temperature of 295 K in the mode of exclusion of specular reflectance (Fig. 8a). One can see that for longer wavelengths the spectra of diffusive reflectance coefficient (R_d) are nearly flat. Values of R_d for the plane parallel to c-axis of SbSI are much larger than those for the perpendicular plane. R_d in this region is dominated by reflection and scattering due to the refractive index of the investigated material. With decreasing the wavelength of radiation one can observe abrupt decrease in R_d (Fig. 8a). It happens when radiation becomes more intensively absorbed with
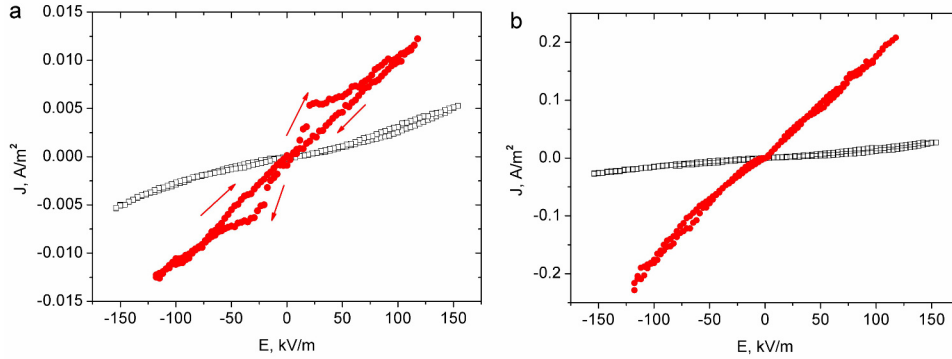
Fig. 6. Current density as a function of electric field intensity in SbSI single crystals at temperatures 283 K (a) and 333 K (b) for different orientations of electric field relative to c-axis (E∥c (●); E⊥c (□); description in the text).
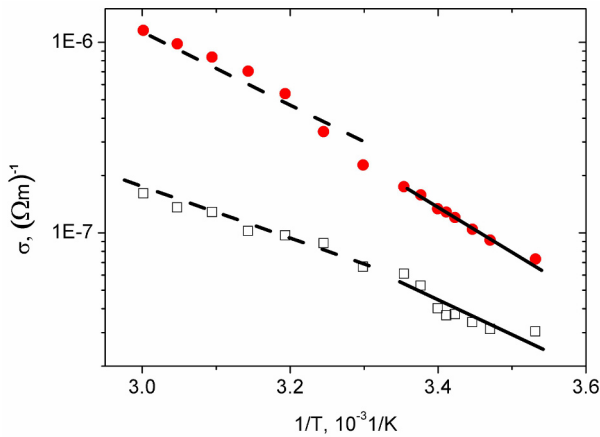

Fig. 7. Electrical conductivity vs. temperature of SbSI single crystals for different orientations of electric field (● – E∥c; □ – E⊥c; solid and dash lines represent Arrhenius dependences fitted in cases of ferroelectric and paraelectric phases).

increasing photon energies (it corresponds to the optical absorption edge). In the range of strong absorbance the spectra of R_d are similar for the both investigated surfaces of SbSI crystal.

The diffuse reflectance values have been converted to the Kubelka-Munk function vs. photon energy (hν) [38]:

$$F_{KM}\left[R_d\left(h\nu\right)\right] = \frac{\left[1 - R_d\left(h\nu\right)\right]^2}{2R_d\left(h\nu\right)} = \frac{\alpha(h\nu)}{S} \quad (1)$$

where α is an absorption coefficient of light in the investigated material, S is a constant scattering factor.

The value of E_g has been determined by the intersection point (Fig. 8b) between lines that extrapolate F_{KM} values in the small hν range and at the linear absorption edge. The values of $E_g = 1.68$ eV and $E_g = 1.87$ eV have been established for the plane perpendicular and parallel to c-axis of SbSI, respectively.

Specular reflectance of the plane perpendicular to c-axis of the SbSI crystal has been measured in spectral range from 380 nm to 1050 nm at room temperature. The scheme of experimental setup has been presented in [39, 40]. The sample was mounted on the table of GUR-5 (LOMO) goniometer. The optical reflectance has been measured using PC2000 (Ocean Optics Inc.) spectrophotometer with master card (600 lines grating, blazed at 500 nm). The spectrophotometer was equipped with appropriate waveguide cables and the deuterium-halogen light source DH2000-FHS from Ocean Optics Inc. The multiple averaged spectral characteristics containing 2048 data points for various wavelengths were registered using the OOI-Base program from Ocean Optics Inc. The measurements were carried out for different angles of light incidence upon a sample. Using Glan-Thomson polarizer (LOT-Oriel) the incoming radiation was linearly polarized with the electric vector parallel "p" or perpendicular "s" to the plane of incidence. Results of specular reflectance for both light polarizations are presented in Fig. 9a and 9b, respectively.
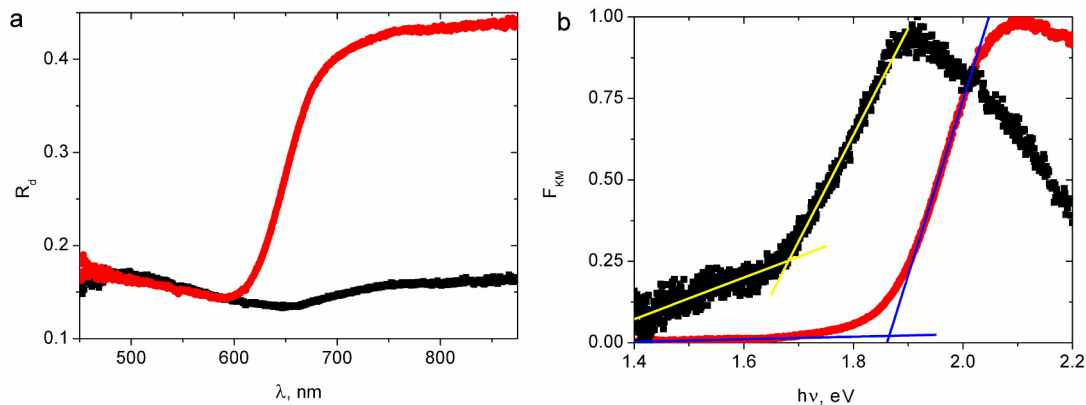
Fig. 8. Spectra of the diffuse reflectance (a) and the determined normalized Kubelka-Munk function (b) for different planes of SbSI single crystal (■, ● – a plane perpendicular and parallel to c-axis of SbSI, respectively).
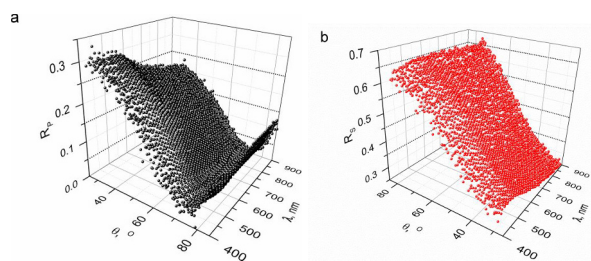

Fig. 9. Angular and spectral dependencies of specular reflectance of a plane perpendicular to c-axis of the SbSI crystal (R_P, R_S – results were registered for a plane polarized radiation with electric field parallel and perpendicular to the plane of incidence, respectively).
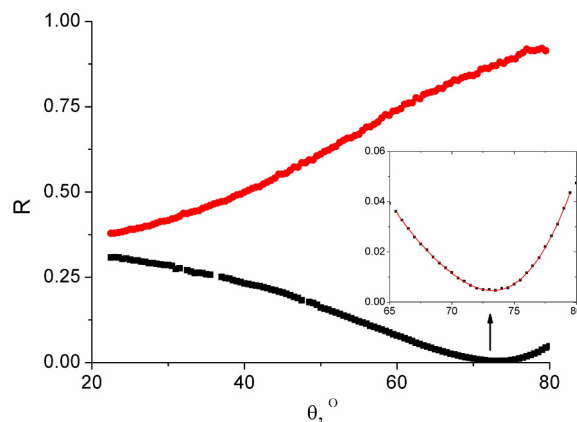

Fig. 10. Angular dependencies of specular reflectance of a plane perpendicular to c-axis of the SbSI crystal for a plane polarized radiation with electric field parallel (■) and perpendicular (●) to the plane of incidence ($\lambda = 600$ nm). The inset shows the neighbourhood of Brewster's angle.

Fig. 10 shows typical angular dependencies of specular reflectance of a plane perpendicular to c-axis of the SbSI crystal for plane polarized radiation with electric field parallel and perpendicular to the plane of incidence. The observed Brewster's angle can be used to determine the real part of refractive index of the investigated crystal. Analysis of the spectral dependences of various components of refractive index of optically anisotropic SbSI crystal is currently in progress and will be presented in the near future.

3. Conclusion

The sonochemically produced SbSI gel consisting of nanowires can be effectively used as a source material in a vapour growth process of SbSI single crystals. The pendulum-heating of the crystallization zone is useful for the growth of large SbSI crystals.

Due to big size and good quality of the front plane perpendicular to c-axis of SbSI crystal, the measurements of angular spectra dependencies of specular reflectance have been performed. Based on the obtained results, anisotropic optical properties, such as ordinary and extraordinary values of refractive index, have been determined.

Large SbSI crystals should receive considerable attention from the scientific and engineering communities due to their potentially useful

applications. They have potentially great importance, e.g. for production of IR sensors, variable focal mirrors and piezoelectric actuators.

References

[1] FRIDKIN V.M., *Photoferroelectrics*, Springer-Verlag, New York, 1979.

[2] FRIDKIN V.M., *Ferroelectric semiconductors*, Consultants Bureau, New York 1980.

[3] GERZANICH E.I., FRIDKIN V.M., *$A_5B_6C_7$ type ferroelectrics*, Nauka, Moscow, 1982 (In Russian).

[4] GERZANICH E.I., LYAKHOVITSKAYA V.A., FRIDKIN V.M., POPOVKIN B.A., *Current topics in materials science 10*, North-Holland, Amsterdam, 1982.

[5] SAWAGUCHI E., HELLWEGE K-H., HELLWEGE A.M., *Landolt-Börnstein III/16b*, Springer-Verlag, Berlin, 1982.

[6] DITTRICH H., KARL N., KŰCK S., SCHOCK W., MADELUNG O., *Landolt-Börnstein Condensed Matter III/41E*, Springer-Verlag, Berlin, 2000.

[7] CHO I., MIN B.-K., JOO S.W., SOHN Y., *Mater. Lett.*, 86 (2012), 132.

[8] VARGHESE J., O'REGAN C., DEEPAK N., WHATMORE R.W., HOLMES J.D., *Chem. Mater.*, 24 (2012), 3279.

[9] NOWAK M., BOBER Ł., BORKOWSKI B., KĘPIŃSKA M., SZPERLICH P., STRÓŻ D., SOZAŃSKA M., *Opt. Mater.*, 35 (2013), 2208.

[10] AUDZIJONIS A., ŽIGAS L., ŽALTAUSKAS R., SEREIKA R., *J. Phys. Chem. Solids*, 75 (2014), 194.

[11] NOWAK M., MISTEWICZ K., NOWROT A., SZPERLICH P., JESIONEK M., STARCZEWSKA A., *Sensor. Actuat. A-Phys.*, 210 (2014), 32.

[12] NOWAK M., NOWROT A., SZPERLICH P., JESIONEK M., KĘPIŃSKA M., STARCZEWSKA A., MISTEWICZ K., STRÓŻ D., SZALA J., RZYCHOŃ T., TALIK E., WRZALIK R., *Sensor. Actuat. A-Phys.*, 210 (2014), 119.

[13] TOROŃ B., NOWAK M., KĘPIŃSKA M., GRABOWSKI A., SZALA J., SZPERLICH P., MALKA I., RZYCHOŃ T., *Opt. Laser. Eng.*, 55 (2014), 232.

[14] LI J.-F., VIEHLAND D., BHALLA A.S., CROSS L.E., *J. Appl. Phys.*, 71 (1992), 2106.

[15] KOTRU S., LIU W., PANDEY R.K., ISAF 2000. *Proceedings of the 2000 12th IEEE International Symposium on Applications of Ferroelectrics (IEEE Cat. No.00CH37076). IEEE, Part 1*, Piscataway, New Jersey, 2001.

[16] SONG X., HANNAN M.A., KOTRU S., PANDEY R.K., *Proc. 10th European Meeting on Ferrolelectricity*, (2003), 316.

[17] PANDEY R.K., KOTRU S., XIUYU S., DONNELLY D., *American Physical Society, March Meeting 2004*, Montreal, Canada, abs. P21.006.

[18] ZEINALLY A.KH., MAMEDOV A.M., *Optiko-Mekhanicheskaya Promyshlennost*, 42 (1975), 72.

[19] HIGUMA Y., MATSUI Y., OKUYAMA M., HAMAKOWA Y., NAKAGAWA T., *Jpn. J. Appl. Phys.*, 17 (1977), 209.

[20] SURTHI S.R., KOTRU S., PANDEY R.K., *Mat. Res. Soc. Symp. Proc.*, 699 (2002), 243.

[21] BETSA V.V., POPIK Y.V., *Fizika Tverdogo Tela*, 19 (1977), 278.

[22] GREKOV A.A., DANILOVA S.P., ZAKS P.L., KULIEVA V.V., RUBANOV L.A., SYRKIN L.N., CHEKHUNOVA N. P., ELGARD A.M., *Akusticheskii Zurnal*, 19 (1973), 622.

[23] NAKONECHNYI Y.S., TURYANITSA I.D., *Fizika Tverdogo Tela*, 16 (1974), 2365.

[24] ARAKELYAN G.K., LYAKHOVITSKAYA V.A., SPITSINA V.D., FREMD V.M., *Seismicheskie Pribory: Instrumentalnaye Sredstva Seismicheskikh Nablyudenii*, 13 (1980), 63.

[25] ALEXANDRAKIS G.C., RITTENMYER K.M., DUBBELDAY P.S., *J. Acoust. Soc. Am.*, 80 (1986), S69.

[26] RITTENMYER K.M., ALEXANDRAKIS G.C., DUBBELDAY P.S., *J. Acoust. Soc. Am.*, 84 (1988), 2002.

[27] GREKOV A.A., KORCHAGINA N.A., ROGACH E.D., *Prib. Tekh. Eksp.*, 22 (1979), 262.

[28] TOROŃ B., NOWAK M., GRABOWSKI A., KĘPIŃSKA M., SZALA J., RZYCHOŃ T., *Proc. SPIE*, 8497 (2012), 84971K-1.

[29] GERZANICH E.I., LYAKHOVITSKAYA V.A., FRIDKIN V.M., POPOVKIN B.A., *Current topics in materials science 10*, North-Holland, Amsterdam, 1982.

[30] OKAZAKI K., *ISAF '96. Proceedings of the Tenth IEEE International Symposium on Applications of Ferroelectrics*, 2 (1996), 779.

[31] GUPTA P., STONE A., WOODWARD N., DIEROLF V., JAIN H., *Opt. Mater. Express*, 652 (2011), 1.

[32] NOWAK M., KAUCH B., SZPERLICH P., STRÓŻ D. SZALA J., RZYCHOŃ T., BOBER Ł., TOROŃ B., NOWROT A., *Ultrason. Sonochem.*, 17 (2010), 487.

[33] NOWAK M., *Photoferroelectric nanowires*, in: LUPU N. (Ed.), *Nanowires Science and Technology*, InTech, Rijeka, 2010.

[34] NEELS H., SCHMITZ W., HOTTMANN H., ROSSNER R., TOPP W., *Kristal und Technik*, 6 (1971), 225.

[35] BOUREGBA R., POULLAIN G., *J. Appl. Phys.*, 93 (2003), 522.

[36] NOWAK M., SZPERLICH P., *Opt. Mater.*, 35 (2013), 1200.

[37] PINTILIE L., VREJOIU I., HESSE D., LERHUN G., ALEXE M., *Phys. Rev. B*, 75 (2007), 104103 1.

[38] NOWAK M., KAUCH B., SZPERLICH P., *Rev. Sci. Instrum.*, 80 (2009), 046107 1.

[39] KĘPIŃSKA M., NOWAK M., DUKA P., KAUCH B., *Thin Solid Films*, 517 (2009), 3792.

[40] KĘPIŃSKA M., NOWAK M., DUKA P., KOTYCZKA-MORAŃSKA M., SZPERLICH P., *Opt. Mater.* 33 (2011) 1753.